

Markus Peura*

Finnish Meteorological Institute

1. INTRODUCTION

In addition to estimating precipitation, Doppler weather radars are routinely used for measuring winds. The most popular wind products are Velocity Azimuth Display (VAD) providing a nearly horizontal intersection of wind field and Velocity Volume Processing (VVP) which averages horizontal wind at altitude ranges above the radar (Fig. 1).

However, perceiving actual wind field by visual inspection of VAD requires some experience. This is due to well-known limitations of Doppler. Firstly, winds are projected on the radar beam, hence reduced to one dimension. Second, the observable speed range is limited by Nyquist velocity $V_n = \lambda F/4$ where λ is the wavelength and F the pulse repetition frequency of the radar. Values exceeding range $[-V_n, +V_n]$ become hence wrapped around ie. aliased, appearing as abrupt jumps of $\pm 2V_n$ in data. These limitations affect also computation of further products.

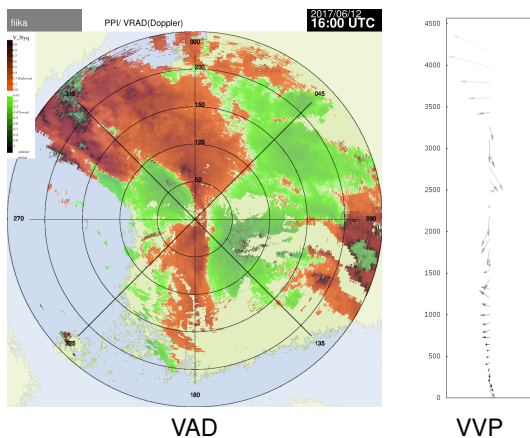


FIG. 1: Conventional Doppler products.

Several algorithms for dealiasing Doppler data has been suggested, for example based on cancelling velocity jumps in areas of connected bins (Jing and Wiener, 1993). In this paper, we present a solution for approximating two-dimensional wind field from the azimuthal derivatives of aliased Doppler winds. Our approach resembles that of Haase and Landelius (2004), where measured wind and azimuth are mapped on a torus and the best-matching order of aliasing is obtained through differentialization. In our approach, the two-dimensional wind is solved directly by inverting a matrix of *continuously accumulated differentials*. We have used this

* Corresponding author address: Markus Peura, Finnish Meteorological Institute, P.O.BOX 503, FIN-00101 Helsinki, Finland; first.name.lastname@fmi.fi

kind of *sliding window* technique also earlier in detecting motion (Peura and Hohti, 2004) and birds (Peura and Koistinen, 2016) in radar.

2. THE PROPOSED METHOD

Essentially, our approach is based on observing *changes* instead of absolute values of Doppler wind. First, consider the Doppler fields of Fig. 2. For this illustration, synthesised fields have been generated for a constant wind \mathbf{v} (from south-west). If the wind is within the Nyquist velocity range $[-V_n, +V_n]$, no aliasing takes place and the wind only gets projected on radar beams, generating a single line of zero speed area (white). For higher-velocity winds, projected speeds will be aliased ie. wrapped around the Nyquist velocity range. Crossings of the range appear as dark areas in this illustration. New (faulty) zero speed lines will appear as well. What is essential for the proposed algorithm, the *azimuthal change rates* in Doppler field reflect the magnitude and direction of the true wind field.

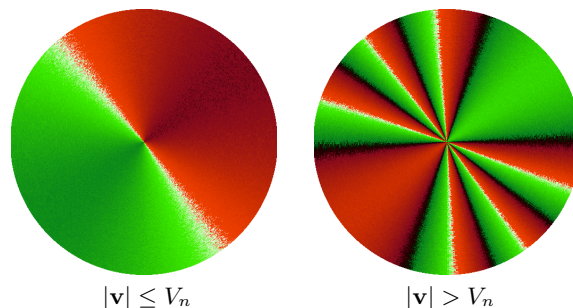


FIG. 2: Doppler fields of constant wind speed within (left) and beyond (right) Nyquist velocity range.

Consider wind $\mathbf{v} = [u \ v]^T$ observed with radar using a low elevation angle. Let us model a radar beam at azimuthal direction α as unit vector $\mathbf{b}(\alpha) = [\cos \alpha \ \sin \alpha]^T$. (In low elevation angles we can omit the vertical component.) Observed wind v_b is the component projected on the beam:

$$v_b(\alpha) = \mathbf{v}^T \mathbf{b}(\alpha) = u \cos \alpha + v \sin \alpha. \quad (1)$$

This is illustrated in Fig. 3. Next, consider the rate of the observed beam-to-beam change in projected wind, here denoted as

$$d = \frac{v_b(\alpha_2) - v_b(\alpha_1)}{\alpha_2 - \alpha_1} = \frac{\Delta v_b}{\Delta \alpha}. \quad (2)$$

Notice that since azimuthal resolution $\Delta \alpha$ is typically around one degree, the *changes* of v_b are small compared to absolute values. Hence, crossing Nyquist velocity range $[-V_n, +V_n]$ in computing Δv_b can be handled safely.

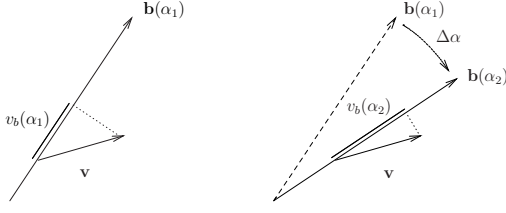


FIG. 3: Observing change Δv_b as a function of azimuth angle α .

In our approach, the basic idea is to match d against the theoretical derivative of beam projected wind v_b :

$$d \approx \frac{\partial v_b}{\partial \alpha} = -u \sin \alpha + v \cos \alpha \quad (3)$$

A critical assumption is that the wind field be locally smooth. Then, we can find wind $\mathbf{v} = [u \ v]^T$ that best explains the changes of beam-projected speed in a local window. Assume Doppler measurements inside a window of $m \times n$ radar bins, with range coordinates r_i , $i \in \{1, 2, \dots, m\}$ and azimuthal coordinates α_j , $j \in \{1, 2, \dots, n\}$. This is illustrated in Fig. 4. Practically, we have noticed that the window should be azimuthally wide, some tens of degrees, whereas a couple of kilometers in range are sufficient.

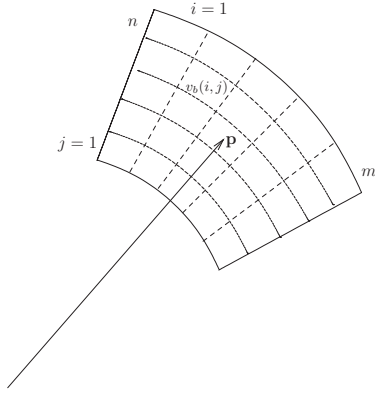


FIG. 4: A Doppler window Ω of $m \times n$ bins around bin position vector \mathbf{p} .

At each bin, this leads to solving a set of $m \times n$ equations, in matrix form minimizing $|\mathbf{e}|$ in

$$\begin{bmatrix} d_{1,1} \\ d_{2,1} \\ \vdots \\ d_{1,2} \\ d_{2,2} \\ \vdots \\ d_{m,n} \end{bmatrix} - \begin{bmatrix} -\sin \alpha_1 & \cos \alpha_1 \\ -\sin \alpha_1 & \cos \alpha_1 \\ \vdots & \vdots \\ -\sin \alpha_2 & \cos \alpha_2 \\ -\sin \alpha_2 & \cos \alpha_2 \\ \vdots & \vdots \\ -\sin \alpha_n & \cos \alpha_n \end{bmatrix} \begin{bmatrix} u \\ v \end{bmatrix} = \mathbf{d} - \mathbf{T}\mathbf{v} = \mathbf{e} \quad (4)$$

where $\mathbf{v} = [u \ v]^T$ is unknown. Its minimum squared-error approximation is

$$\hat{\mathbf{v}} = (\mathbf{T}^T \mathbf{T})^{-1} \mathbf{T}^T \mathbf{d} \quad (5)$$

Rewriting the column vectors of \mathbf{T} in (4) as $\mathbf{T} = [\mathbf{s} \ \mathbf{c}]$ we get

$$\hat{\mathbf{v}} = \begin{bmatrix} \mathbf{s}^T \mathbf{s} & \mathbf{s}^T \mathbf{c} \\ \mathbf{c}^T \mathbf{s} & \mathbf{c}^T \mathbf{c} \end{bmatrix}^{-1} \begin{bmatrix} \mathbf{s}^T \\ \mathbf{c}^T \end{bmatrix} \mathbf{d} \quad (6)$$

which involves an inversion of a 2×2 matrix easily written out

$$\hat{\mathbf{v}} = \frac{1}{(\mathbf{s}^T \mathbf{s})(\mathbf{c}^T \mathbf{c}) - (\mathbf{c}^T \mathbf{s})^2} \begin{bmatrix} \mathbf{c}^T \mathbf{c} & -\mathbf{c}^T \mathbf{s} \\ -\mathbf{c}^T \mathbf{s} & \mathbf{s}^T \mathbf{s} \end{bmatrix} \begin{bmatrix} \mathbf{s}^T \mathbf{d} \\ \mathbf{c}^T \mathbf{d} \end{bmatrix}. \quad (7)$$

Hence, this approximates original wind at a given radar bin. However, if a radar sweep consists of M rays, each having N range bins, and the computational window covers m rays and n range bins, the overall computational effort involves order of $M \times N \times m \times n$ steps – for example $500 \cdot 360 \cdot 90 \cdot 5 \approx 8,000,000$ operations – which is easily unfeasible. Luckily, the computation can be accelerated, as explained next.

3. SLIDING WINDOWS – SPEED THROUGH ACCUMULATION

First, consider a simpler problem: smoothing image f of size $M \times N$ with an averaging window Ω of size $m \times n$. In the smoothed image, each pixel is assigned the average intensity $f(k, l) = \frac{1}{mn} \sum_j \sum_i f(k+i, l+j)$. If computational effort is of no concern, the average could be computed over and over in each pixel, resulting in $M \times N \times m \times n$ operations. On the other hand, the average can be also computed cumulatively: when the window is moved one step, one column of elements is subtracted and one column is added in the sum, resulting in $M \times N \times n$ operations. This "pipeline" approach is illustrated in Fig. 5.

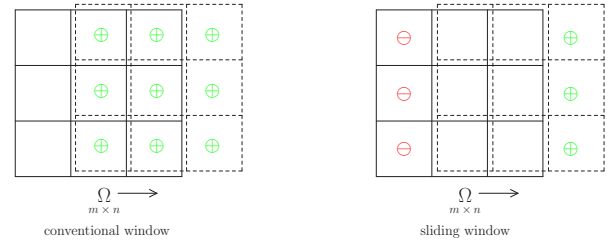


FIG. 5: In the sliding approach, traversing the $m \times n$ elements (left) are replaced with n subtractions and n additions (right). Additions and subtractions are marked with \oplus and \ominus , respectively.

In addition to computing averages, all the statistics which can be derived from accumulated values are suited to pipeline architecture. For example, also variance can be computed using accumulated values as follows:

$$\sigma^2 = \frac{1}{N} \sum (x - \mu_x)^2 = \frac{1}{N} \sum x^2 - \mu_x^2. \quad (8)$$

One can design the computation such that the statistics are initialized only once, in the starting corner of image traversal. This leads to forth-and-back row traversal illustrated in Fig. 6.

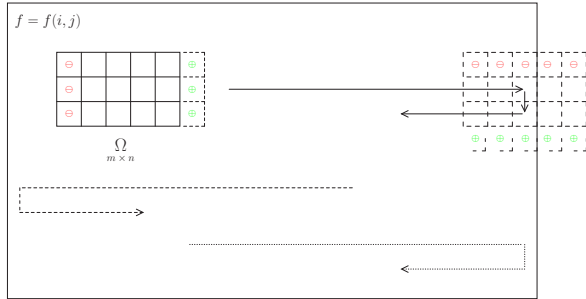


FIG. 6: A sliding window Ω traverses each row (or column) in the image once, reversing the direction at the image edges. To minimize computational effort, a non-square ($m \neq n$) window should move shorter edge facing the main direction.

The solution for Doppler wind retrieval (7) involves five summations that can be accumulated continuously: $c^T c$, $c^T s$, $s^T s$, $s^T d$, and $c^T d$. This means that sliding window technique can be applied for solving $\mathbf{v} = [u \ v]^T$ quickly for each bin of a radar sweep.

4. EXAMPLE

A result of the proposed (u, v) retrieval algorithm for a single radar is shown in Fig. 7 (FMI Kuopio radar, 2017/06/12 16:00 UTC). The applied window size was 90 degrees (90 bins) and 5km (10 bins). The algorithm produces also a quality (certainty) measure of the retrieved field, defined as the determinant of the matrix inversion: $|\mathbf{T}^T \mathbf{T}| = (s^T s)(c^T c) - (c^T s)^2$. The quality is illustrated as opacity of arrows. Apparently, the algorithm performs well in large areas but is sensitive to noise in small areas. Also, far from radar the algorithm provides wind approximations of lower quality. This is probably due to relatively larger area and hence, larger variability in wind. On the other hand, wind vectors far from the radar can be expected be larger as they originate from bins higher in the atmosphere.

Further, the wind fields retrieved separately for all the FMI radars have been composited using quality-weighted average. As input quality, determinant as well as fuzzy weighting of height has been applied. The result is shown in Fig. 8.

5. CONCLUSIONS

We presented a fast wind retrieval method in which the basic idea is to find (u, v) that best explains the observed local azimuthal speed change. The involved least-squares fitting is computed in original polar coordinates using a two-dimensional neighborhood window. The size of the window should be relatively large in azimuthal direction, for example 60 or 90 degrees, whereas rather small beam-directional range, say 3–5 kms, seems sufficient.

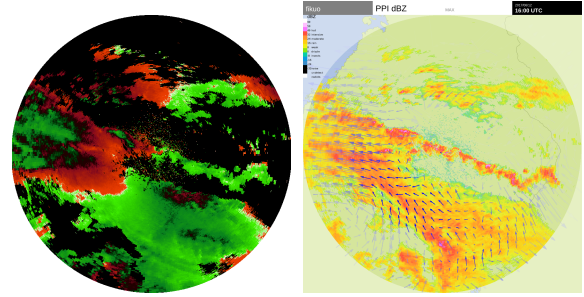


FIG. 7: Original Doppler field (left) as well as the corresponding retrieved wind field superposed on reflectivity of the lowest (0.5°) elevation of FMI Kuopio radar on 2017/06/12 16:00 UTC.

The proposed method is rather insensitive to small Nyquist velocities. The reason is in that also for strong winds the observed changes of speed in azimuthal direction are much smaller than the (unambiguous) speed range, hence differences can be treated unaliased. However, the algorithm fails in convective precipitation, as velocity field becomes noisy inside the sliding window.

This proposed quick computation of wind fields can be utilized directly in meteorological image products as well as in computation of extrapolation based forecasts.

REFERENCES

- Haase, G. and T. Landelius, 2004: Dealiasing of doppler radar velocities using a torus mapping. *Journal of Atmospheric and Oceanic Technology*, **21**(10), 1566–1573.
- Jing, Z. and G. Wiener, 1993: Two-dimensional dealiasing of doppler velocities. *Journal of Atmospheric and Oceanic Technology*, **10**(6), 798–808.
- Peura, M., 2012: Rack - a program for anomaly detection, product generation, and compositing. In *7th European Conference on Radar in Meteorology and Hydrology (ERAD2012)*, Météo France. Software can be downloaded from <https://github.com/fmidev/rack>.
- Peura, M. and H. Hohti, 2004: Optical flow in radar images. In *Third European Conference on Radar in Meteorology and Hydrology (ERAD2004)*, Copernicus, 454-458.
- Peura, M. and J. Koistinen, 2016: Fuzzy logic based spatial bird detection with weather radar. In *Proceedings of the 9th European Conference on Radar in Meteorology and Hydrology (ERAD2016)*.

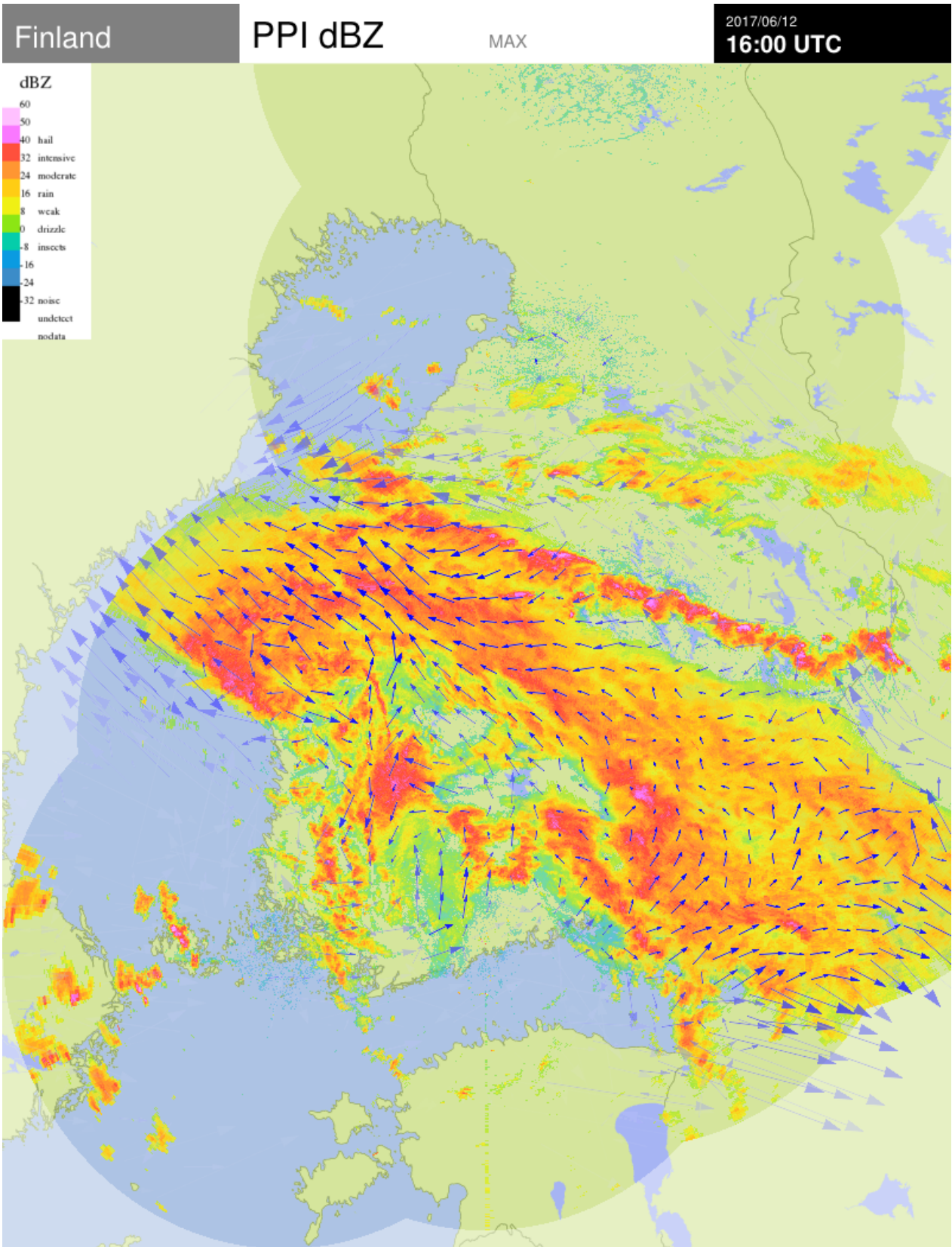


FIG. 8: Wind field $\mathbf{v} = [u \ v]^T$ obtained as quality-weighted composite of wind fields solved separately for each radar.